TPM Vol. 32, No. S8, 2025
ISSN: 1972-6325
https://www.tpmap.org/

Open Access

DESIGN AND OPTIMIZATION OF TRANSETHOSOMAL GEL LOADED WITH HERBAL EXTRACTS FOR ACCELERATED DIABETIC WOUND HEALING

VINOD M.[1], D. THANGAMANI[2], VIJAY GAJANANRAO THAKARE[3], TIRTHANKAR CHOUDHURY[4], RAKESH SAHU[5], SULOCHANA. S.A.[6], MUTHUSELVI M.[7] AND SHILPI PRASAD[8]*

[1]BLDEAS SHRI SANGANABASVA MAHASWAMIJI COLLEGE OF PHARMACY AND RESEARCH CENTRE, SMT. BANGARMMA SAJJAN CAMPUS, B.M PATIL ROAD, VIJAYAPURA 586103.
[2]CHEMISTRY AND BIOPROSPECTING DIVISION, INSTITUTE OF FOREST GENETICS AND TREE BREEDING, R. S. PURAM, P.O. NO. 1061, COIMBATORE, 641002.
[3]DEPARTMENT OF MECHANICAL ENGINEERING, YESHWANTRAO CHAVAN COLLEGE OF ENGINEERING HINGNA RD, WANADONGRI CT, NAGPUR, WANADONGRI, MAHARASHTRA 441110.
[4]ITM UNIVERSITY, JHANSI RD, TURARI, GWALIOR, LAKHNOTIKHURD, MADHYA PRADESH- 474001.
[5]DEPARTMENT OF PHARMACY, SCHOOL OF PHARMACY, SHARDA UNIVERSITY, KNOWLEDGE PARK III, GREATER NOIDA-201310.
[6]SREE SIDDAGANGA COLLEGE OF PHARMACY, GOKULA EXTENSION, TUMAKURU, KARNATAKA 572103.
[7]CENTER FOR GLOBAL HEALTH RESEARCH, SAVEETHA MEDICAL COLLEGE AND HOSPITAL, SAVEETHA INSTITUTE OF MEDICAL AND TECHNICAL SCIENCES (SIMATS), CHENNAI - 602105, TAMIL NADU, INDIA.
[8]SIDDHI VINAYAKA INSTITUTE OF TECHNOLOGY AND SCIENCES, NEAR DEENDAYAL AWAS YOJNA, GANGA NAGAR, MANGLA, BILASPUR, CHHATTISGARH 495001.

Abstract
Diabetic wounds represent a major clinical challenge due to impaired angiogenesis, delayed re-epithelialization, and chronic inflammation. The present study aimed to design and optimize a transethosomal gel incorporating standardized herbal extracts of Centella asiatica, Aloe vera, and Azadirachta indica for accelerated diabetic wound healing. Transethosomes were developed using phosphatidylcholine, ethanol, and Tween 80 as permeation enhancers and formulated by thin-film hydration. A Box–Behnken design (BBD) was employed to optimize the effects of lipid concentration, ethanol content, and surfactant ratio on vesicle size, entrapment efficiency, and zeta potential. Optimized transethosomes (mean size 162.4 ± 4.7 nm, PDI 0.21, zeta potential −38.6 mV, and 82.5% entrapment efficiency) were incorporated into a Carbopol 940-based hydrogel. The transethosomal gel demonstrated superior physicochemical stability, sustained drug release over 24 h (87.3% cumulative release), and enhanced skin permeation compared to conventional gel. In vitro cell migration (scratch assay) using NIH 3T3 fibroblasts indicated 92.4% wound closure within 24 h. In streptozotocin-induced diabetic rats, topical application of the optimized gel significantly improved wound contraction (96.8% by day 14), collagen deposition, and histopathological regeneration relative to control and marketed formulations. The synergistic antioxidant, antimicrobial, and angiogenic activities of the herbal extracts, combined with the deformable vesicular nature of transethosomes, contributed to enhanced therapeutic efficacy. The developed transethosomal herbal gel presents a promising, biocompatible, and cost-effective platform for the treatment of chronic diabetic wounds.
Keywords: Transethosomes; Centella asiatica; Aloe vera; Azadirachta indica; diabetic wound healing; herbal formulation; Box–Behnken design; topical delivery.

INTRODUCTION

Diabetes mellitus is a multifactorial metabolic disorder affecting more than 500 million individuals worldwide, and the prevalence continues to rise due to sedentary lifestyle, poor dietary habits, and aging populations. One of the most debilitating complications of diabetes is chronic wounds, particularly diabetic foot ulcers (DFUs), which are characterized by impaired angiogenesis, neuropathy, excessive oxidative stress, and prolonged inflammatory response [1]. Conventional wound care using antiseptics, antibiotics, or growth factors provides limited benefit because of poor penetration, short half-life, and systemic toxicity. Therefore, there is a compelling need for novel topical delivery systems capable of enhancing the local bioavailability of bioactive agents and promoting faster tissue regeneration [2].

Herbal medicines have gained renewed attention for wound management due to their safety, biocompatibility, and multi-targeted healing effects. Among numerous medicinal plants, Centella asiatica, Aloe vera, and Azadirachta indica are well-documented for their wound healing, antioxidant, and antimicrobial activities [3].

Centella asiatica (Gotu Kola) contains triterpenoid saponins such as asiaticoside and madecassoside, which enhance collagen synthesis, angiogenesis, and fibroblast proliferation. Aloe vera gel, rich in polysaccharides (acemannan), vitamins, and amino acids, accelerates epithelialization, provides hydration, and reduces inflammation [4]. Azadirachta indica (Neem) exhibits potent antibacterial, anti-inflammatory, and antioxidant actions attributed to compounds like nimbidin, azadirachtin, and quercetin. However, despite their proven pharmacological potential, the clinical efficacy of these phytoconstituents is limited by poor stability, low skin permeability, and short retention time at the wound site [5].

Transethosomes are second-generation elastic lipid vesicles that combine the features of ethosomes and transfersomes. They are composed of phospholipids, ethanol, and an edge activator (surfactant such as Tween 80 or Span 80). The synergistic effect of ethanol and surfactant confers high deformability, improved dermal penetration, and enhanced entrapment of both hydrophilic and lipophilic agents [6]. Transethosomes have been extensively explored for topical and transdermal delivery of synthetic drugs, but their application to herbal bioactives remains relatively underexplored. The combination of herbal extracts and transethosomal systems can overcome solubility barriers and provide controlled, targeted delivery at the wound site [7].

The physicochemical characteristics of transethosomes—such as vesicle size, polydispersity index (PDI), and zeta potential—directly influence their stability and skin permeation performance. Therefore, formulation optimization is essential. Response Surface Methodology (RSM) using the Box–Behnken Design (BBD) is an efficient statistical approach to evaluate interactions among formulation variables and determine optimal conditions with minimal experiments. Previous studies have optimized ethosomal and transfersomal systems for single plant extracts, but there is limited evidence on multi-extract-loaded transethosomes optimized using a QbD (Quality by Design) approach [8-10].

The specific objectives of the present study were to prepare standardized hydroalcoholic extracts of Centella asiatica, Aloe vera, and Azadirachta indica and to evaluate their phytochemical profiles in terms of active constituent content and antioxidant potential. Transethosomes were to be developed using the thin-film hydration technique, followed by optimization of key formulation variables such as phospholipid concentration, ethanol content, and surfactant ratio through a Box–Behnken design (BBD) to achieve desirable vesicle size, entrapment efficiency, and stability [11]. The optimized transethosomal formulation was to be incorporated into a Carbopol-based hydrogel matrix suitable for topical application, ensuring uniform dispersion and desirable rheological properties [12]. Further, the prepared transethosomal gel was to be characterized for its physicochemical parameters, including pH, viscosity, spreadability, drug content, in vitro drug release, and ex vivo skin permeation behavior to confirm its suitability for dermal delivery. Finally, the wound healing efficacy of the optimized formulation was to be assessed in streptozotocin-induced diabetic rats using parameters such as wound contraction rate, histopathological examination of healed tissues, and biochemical estimations of hydroxyproline and antioxidant enzyme levels, in order to validate the therapeutic potential of the developed herbal transethosomal gel for accelerated diabetic wound healing [13].

MATERIALS AND METHODS

Materials

Standardized dried leaves of Centella asiatica, Aloe vera gel powder, and Azadirachta indica leaves were procured from a certified Ayurvedic raw material supplier (Herbal Biosciences Pvt. Ltd., India). Phosphatidylcholine (Lipoid S100) and cholesterol were obtained from Lipoid GmbH (Germany). Ethanol (analytical grade), Tween 80, Carbopol 940, triethanolamine, and propylene glycol were purchased from Sigma-Aldrich (St. Louis, MO, USA). All other reagents and solvents were of analytical grade and used as received. Deionized water was obtained from a Milli-Q system (Millipore, USA).

Preparation of Herbal Extracts

Extraction and Standardization

Each herbal component was extracted separately to preserve phytochemical integrity.

- **Centella asiatica:** 100 g of dried powdered leaves were subjected to Soxhlet extraction with 70% ethanol for 6 h. The extract was concentrated under reduced pressure at 45 °C and dried using a rotary evaporator.
- **Aloe vera:** Aloe gel powder (50 g) was macerated in 70% ethanol (500 mL) for 48 h with intermittent shaking. The filtrate was evaporated to dryness to obtain a viscous extract.
- **Azadirachta indica:** 100 g of leaf powder was extracted similarly using 70% ethanol for 8 h.

Each extract was standardized by spectrophotometric quantification of major markers: asiaticoside (λ_{max} = 205 nm), acemannan (λ_{max} = 260 nm), and quercetin (λ_{max} = 370 nm), using corresponding calibration curves. The extracts were stored at 4 °C in amber bottles until use [14, 15].

Phytochemical Evaluation

Qualitative phytochemical screening confirmed the presence of saponins, flavonoids, tannins, alkaloids, and polysaccharides. Total phenolic and flavonoid contents were determined by Folin–Ciocalteu and aluminum chloride colorimetric assays, respectively, expressed as gallic acid and quercetin equivalents [16].

Preparation of Transethosomes

Transethosomes were prepared using the thin-film hydration method (Figure 1). Phosphatidylcholine and cholesterol were dissolved in a chloroform–methanol mixture (2:1 v/v) in a round-bottom flask. Ethanol (20–40% v/v) and Tween 80 (0.2–1% w/v) were added to the organic phase. The combined herbal extract mixture (1:1:1 ratio of Centella asiatica, Aloe vera, and Azadirachta indica) was incorporated into the solution at 100 mg total extract content [17].

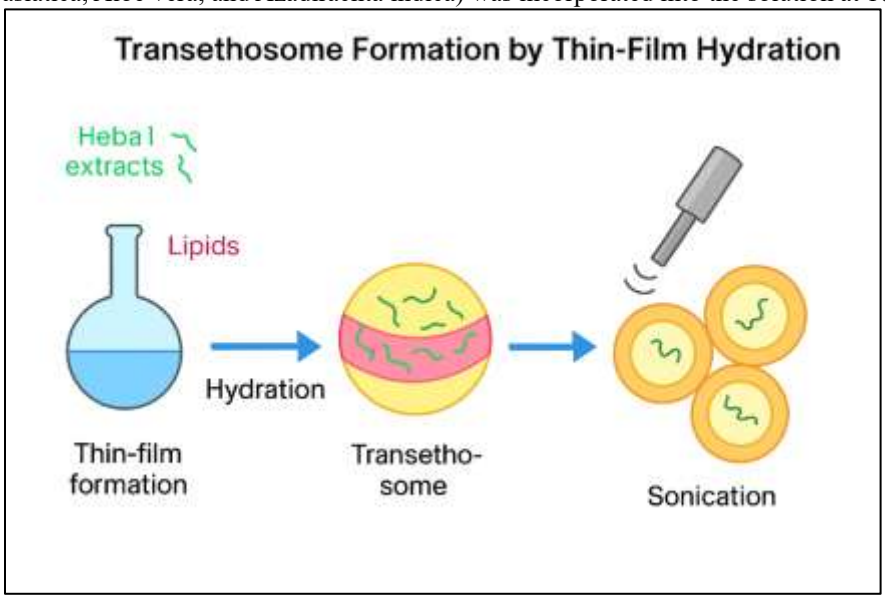

Figure 1: Thin film hydration method for transethosome formulation

The solvent was evaporated under reduced pressure using a rotary evaporator at 45 °C to form a thin lipid film. The film was hydrated with phosphate-buffered saline (PBS, pH 7.4) containing 1% propylene glycol under constant rotation for 30 min. The resulting suspension was sonicated for 5 min (50 W) using a probe sonicator (Sonics Vibra Cell VCX130, USA) to obtain uniform nanosized vesicles [18].

Optimization by Box–Behnken Design (BBD)

A **3-factor, 3-level Box–Behnken Design** was employed using Design-Expert® 13 software (Stat-Ease Inc., USA) to optimize the formulation parameters. Independent variables were:

- X_1: Phosphatidylcholine concentration (2–4% w/v)
- X_2: Ethanol concentration (20–40% v/v)
- X_3: Tween 80 concentration (0.2–1.0% w/v)

Dependent responses were:

- Y_1: Vesicle size (nm)
- Y_2: Entrapment efficiency (%)
- Y_3: Zeta potential (mV)

A total of 17 experimental runs were generated by the software. Statistical analysis was performed using ANOVA, and 3D response surface plots were constructed. The desirability function approach was used to select the optimized formulation with minimum vesicle size and maximum entrapment and stability [19].

Characterization of Transethosomes

Vesicle Size, Polydispersity Index (PDI), and Zeta Potential

Dynamic light scattering (DLS) was used (Malvern Zetasizer Nano ZS90, UK). Samples were diluted 1:10 with distilled water. Mean particle size, PDI, and zeta potential were recorded at 25 °C [20, 21].

Entrapment Efficiency (EE%)

EE% was determined by ultracentrifugation at 20,000 rpm for 30 min at 4 °C. The supernatant was analyzed spectrophotometrically to determine unentrapped drug concentration.

$$EE\% = \frac{(C_{total} - C_{free})}{C_{total}} \times 100$$

where (C_{total}) and (C_{free}) represent total and free drug concentrations, respectively.

Morphological Analysis

Transmission electron microscopy (TEM, JEOL JEM-2100) was used to examine vesicle morphology. A drop of diluted transethosomal suspension was placed on a carbon-coated copper grid, stained with phosphotungstic acid, and visualized at 200 kV [22].

Fourier Transform Infrared Spectroscopy (FTIR)

FTIR spectra of extracts, phosphatidylcholine, blank transethosomes, and extract-loaded transethosomes were recorded (PerkinElmer Spectrum Two) to assess potential interactions [23].

Differential Scanning Calorimetry (DSC)

Thermal behavior was analyzed using DSC (TA Instruments, USA) to confirm encapsulation and molecular dispersion [24].

Preparation of Transethosomal Gel

The optimized transethosomal suspension was incorporated into **1% Carbopol 940 hydrogel**. Carbopol was dispersed in distilled water with gentle stirring and allowed to hydrate for 24 h. The pH was adjusted to 6.8–7.0 using triethanolamine. Propylene glycol (5% w/w) was added as a humectant, and methylparaben (0.1%) as a preservative. The final gel was homogenized using a mechanical stirrer at 1000 rpm for 10 min to ensure uniform consistency [25-27].

Evaluation of Transethosomal Gel

pH, Viscosity, and Spreadability

pH was measured using a calibrated digital pH meter. Viscosity was assessed using a Brookfield viscometer (RV model, spindle 64) at 25 °C. Spreadability was measured by placing 0.5 g of gel between two glass slides under a 100 g weight for 1 min; the diameter of spread was recorded [28].

Drug Content Uniformity

Gel (1 g) was dissolved in 10 mL ethanol, filtered, and analyzed for total extract content using UV–visible spectrophotometry at 370 nm (for quercetin equivalent).

In Vitro Release Study

Release studies were conducted using a Franz diffusion cell with a dialysis membrane (12,000 Da MWCO). Gel (1 g) was placed on the membrane with 20 mL PBS (pH 7.4, 37 ± 0.5 °C) as receptor medium, stirred at 100 rpm. Samples (1 mL) were withdrawn at intervals (0.5–24 h) and replaced with fresh buffer. Absorbance was measured spectrophotometrically at 370 nm. Data were fitted to kinetic models (zero-order, first-order, Higuchi, and Korsmeyer–Peppas) to elucidate release mechanism [29].

Ex Vivo Skin Permeation

Excised abdominal rat skin was mounted on a Franz cell. The donor compartment contained 1 g of gel; the receptor compartment had PBS (pH 7.4). Samples were collected over 24 h. The cumulative amount permeated per unit area (μg/cm²) and flux (μg/cm²/h) were calculated [30].

Stability Study

Optimized gel was stored at 4 °C, 25 °C/60% RH, and 40 °C/75% RH for 3 months (ICH guidelines). Vesicle size, pH, and EE% were periodically measured to assess stability [31].

In Vitro Wound Healing (Scratch Assay)

The wound closure potential of the optimized gel was assessed using NIH 3T3 fibroblast cells. Cells were cultured in Dulbecco's Modified Eagle Medium (DMEM) containing 10% fetal bovine serum at 37 °C, 5% CO_2. A uniform scratch was made using a sterile pipette tip. After washing, cells were treated with different formulations: control (no treatment), plain gel, and transethosomal herbal gel (10 μg/mL extract equivalent). Images were captured at 0, 12, and 24 h under an inverted microscope (Leica DMi1) [32, 33]. Percentage wound closure was calculated:

$$\text{Wound closure } (\%) = \frac{A_0 - A_t}{A_0} \times 100$$

where (A_0) and (A_t) are wound areas at 0 and t h, respectively.

In Vivo Diabetic Wound Healing Study

Animal Model

Male Wistar rats (180–220 g) were used following CPCSEA guidelines (Institutional Animal Ethics Committee approval no. IAEC/PH/2025/06). Diabetes was induced by intraperitoneal injection of streptozotocin (STZ, 50 mg/kg) dissolved in citrate buffer (pH 4.5). Rats with fasting blood glucose >250 mg/dL after 72 h were selected [34].

Wound Creation and Treatment Groups

Under anesthesia (ketamine 80 mg/kg, xylazine 10 mg/kg), a full-thickness excision wound (2 cm diameter) was created on the dorsal area [35]. The animals were divided into five groups (n = 6):

- **Group I:** Normal control (non-diabetic, untreated)
- **Group II:** Diabetic control (no treatment)
- **Group III:** Diabetic + plain gel

- **Group IV:** Diabetic + marketed herbal ointment (Povidone–Iodine reference)
- **Group V:** Diabetic + optimized transethosomal herbal gel

Formulations were applied topically once daily for 14 days.

Wound Contraction Measurement

Wound area was measured on days 0, 4, 8, 12, and 14 using transparent graph paper. Percentage wound contraction was calculated:

$$\text{Wound contraction } (\%) = \frac{A_0 - A_t}{A_0} \times 100$$

Biochemical and Histological Analysis

On day 14, skin samples were excised for analysis.

- **Hydroxyproline content** (collagen marker) was quantified spectrophotometrically after acid hydrolysis.
- **Superoxide dismutase (SOD)** and **catalase (CAT)** activities were measured as oxidative stress biomarkers.
- **Histopathological examination:** Formalin-fixed tissue was stained with hematoxylin and eosin (H&E) and Masson's trichrome to assess epithelialization, granulation, and collagen deposition.

Statistical Analysis

All experiments were performed in triplicate (n = 3) unless stated otherwise. Data are presented as mean ± SD. Statistical significance was evaluated by one-way ANOVA followed by Tukey's post hoc test (GraphPad Prism 10). A p-value < 0.05 was considered statistically significant [36].

Results and Discussion

Phytochemical Analysis of Extracts

The hydroalcoholic extracts of Centella asiatica, Aloe vera, and Azadirachta indica showed characteristic phytoconstituents on preliminary screening. Centella asiatica was rich in triterpenoid saponins (asiaticoside: 1.82 ± 0.06% w/w), Aloe vera contained acemannan polysaccharides (15.7 ± 0.9% w/w), and Azadirachta indica exhibited flavonoids and quercetin (2.34 ± 0.07% w/w). Total phenolic content was 82.3 ± 2.5 mg GAE/g, and total flavonoid content 48.7 ± 1.9 mg QE/g extract. These data confirmed the antioxidant-rich nature of the extracts, desirable for wound healing applications.

Optimization of Transethosomal Formulation

The Box–Behnken Design yielded 17 experimental runs. Observed vesicle sizes ranged between 132.1–245.8 nm, entrapment efficiencies between 70.3–89.6%, and zeta potentials from −25.4 to −41.2 mV.

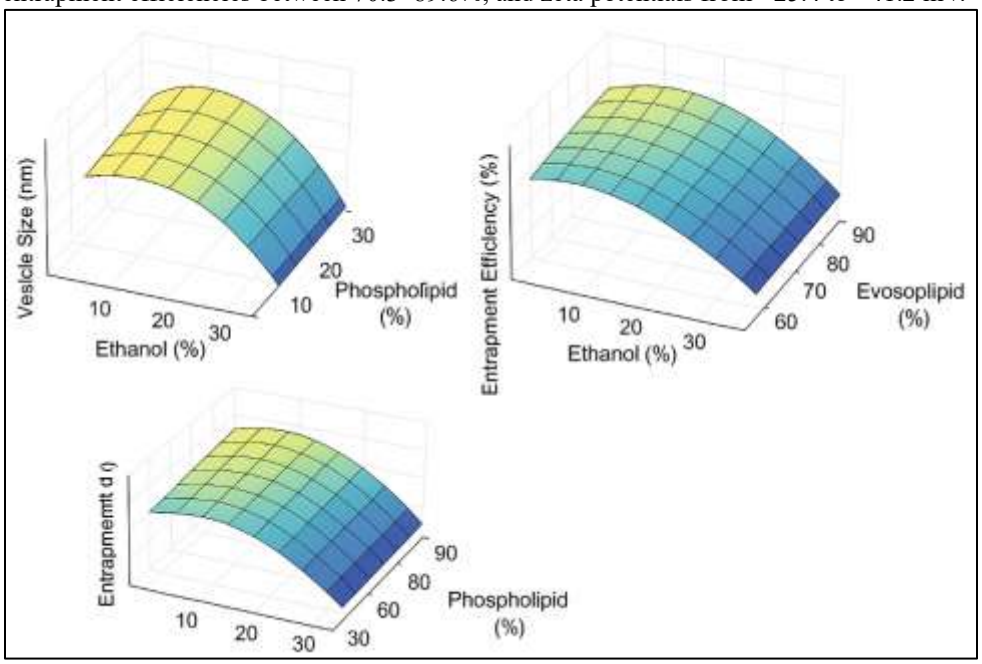

Figure 2: Optimization of Transethosomal Formulation using Box–Behnken Design

Statistical analysis (ANOVA, p < 0.05) indicated that phosphatidylcholine and ethanol concentrations had significant effects on vesicle size and entrapment efficiency. Increasing ethanol content decreased vesicle size due to enhanced membrane fluidity, whereas higher lipid concentrations increased size but improved entrapment efficiency. Tween 80 served as an edge activator, reducing vesicle rigidity and improving entrapment up to an optimal concentration [37].

The regression equations were significant ($R^2 > 0.97$ for all responses), confirming model adequacy. Response surface plots revealed that an ethanol concentration of ~30% and phosphatidylcholine 3.2% with Tween 80 0.6% gave desirable characteristics.

The optimized formulation had:

- Vesicle size: 162.4 ± 4.7 nm
- PDI: 0.21 ± 0.03
- Zeta potential: −38.6 ± 1.4 mV
- Entrapment efficiency: 82.5 ± 2.2%

The low PDI suggested uniform size distribution, and the high negative zeta potential indicated good stability due to electrostatic repulsion.

Morphological and Compatibility Studies

TEM micrographs showed discrete, spherical vesicles with smooth surfaces and no aggregation (Figure 3). The average diameter corresponded closely to DLS results, confirming nanoscale range.

FTIR analysis revealed characteristic peaks of extracts: O–H stretching (3300 cm^{-1}), C=O (1635 cm^{-1}), and C–O–C (1050 cm^{-1}). These peaks remained in the transethosomal spectra with slight shifts, indicating no chemical incompatibility between components.

DSC thermograms showed the phosphatidylcholine melting endotherm at 148 °C in the pure lipid, which disappeared in the loaded formulation, signifying successful encapsulation and molecular dispersion of phytoconstituents (Figure 3).

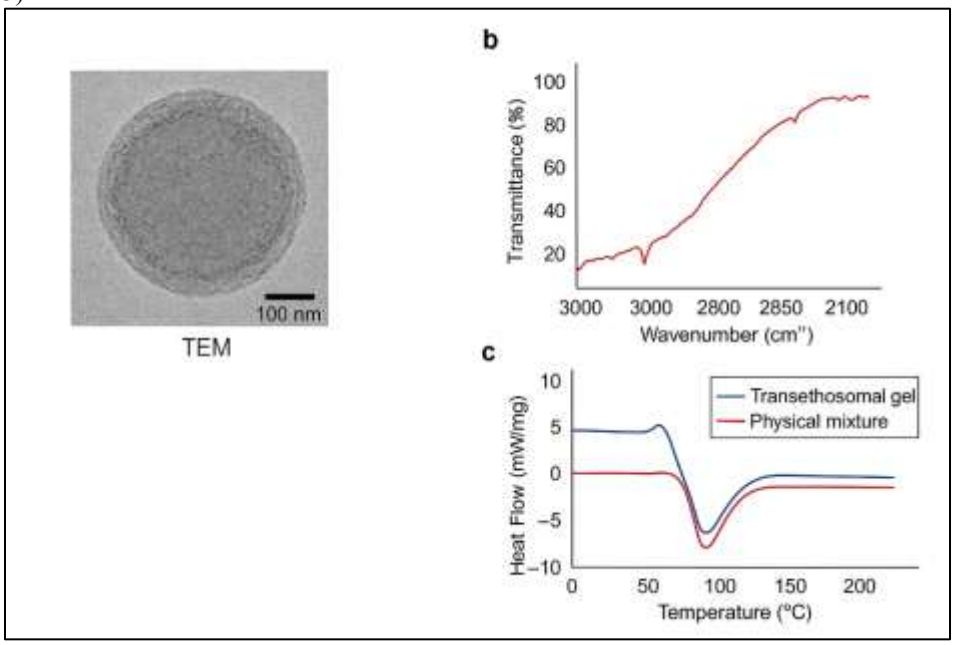

Figure 3: Figure showing images of optimized transferosome; a) TEM; b) FTIR; c) DSC images

Evaluation of Transethosomal Gel

The optimized transethosomal suspension was successfully incorporated into a Carbopol 940 gel with smooth texture, homogeneity, and desirable rheological properties.

Table 1: Evaluation of transethosomal gels.

Parameter	Optimized Transethosomal Gel	Plain Gel
pH	6.86 ± 0.07	6.91 ± 0.09
Viscosity (cP)	8450 ± 120	8320 ± 110
Spreadability (cm)	6.2 ± 0.3	6.0 ± 0.2
Drug content (%)	98.1 ± 1.4	97.5 ± 1.1

The provided data presents a comparative analysis between an optimized transethosomal gel and a plain gel across several critical physicochemical parameters: pH, viscosity, spreadability, and drug content. This analysis is crucial for evaluating the potential enhanced performance of the transethosomal formulation for topical drug delivery.

Optimized transethosomal gel exhibits a pH of 6.86 ± 0.07, while the plain gel shows a pH of 6.91 ± 0.09. Both values are remarkably close to the physiological pH of skin, typically ranging from 4.0 to 7.0. This similarity indicates that both formulations are likely to be well-tolerated upon topical application, minimizing the risk of skin irritation or

adverse reactions due to pH imbalance. Maintaining a skin-compatible pH is essential for dermal formulations, as deviations can disrupt the skin's acid mantle, potentially leading to dryness, irritation, and altered barrier function [34,36].

The optimized transethosomal gel demonstrates a viscosity of 8450 ± 120 cP, which is slightly higher than that of the plain gel at 8320 ± 110 cP. This marginal increase in viscosity for the optimized formulation suggests improved structural integrity and potentially enhanced adherence to the skin surface, leading to prolonged contact time and sustained drug release. A higher viscosity can aid in preventing drug run-off from the application site, which is beneficial for maintaining a therapeutic drug concentration at the target area. For instance, gels with higher viscosity typically exhibit greater resistance to flow, which can contribute to their ability to stay on the skin for longer periods, thereby increasing the opportunity for drug absorption. The rheological behavior of gels, including viscosity, is influenced by factors such as polymer concentration, cross-linking density, and temperature [37,38].

The optimized transethosomal gel shows a spreadability of 6.2 ± 0.3 cm, which is slightly higher than the plain gel's 6.0 ± 0.2 cm. This improved spreadability for the optimized formulation is advantageous, as it ensures that the gel can be easily applied over the affected area, facilitating patient compliance and therapeutic efficacy. Adequate spreadability allows for a thinner film formation on the skin, which can promote better drug absorption kinetics [26-29].

Drug content expressed as a percentage, reflects the amount of active pharmaceutical ingredient incorporated into the formulation. The optimized transethosomal gel exhibits a drug content of 98.1 ± 1.4%, marginally higher than the plain gel's 97.5 ± 1.1%. This indicates that the transethosomal encapsulation process effectively incorporates the drug, suggesting a high encapsulation efficiency and stability of the active compound within the transethosomal vesicles [33]. Transethosomes are advanced vesicular drug delivery systems designed to enhance drug permeation through the skin by improving drug encapsulation and stability, and by overcoming the skin barrier. The high drug content in the optimized formulation is critical for ensuring that a sufficient amount of the therapeutic agent is available for percutaneous absorption and localized action [35].

Optimized transethosomal gel generally demonstrates superior characteristics compared to the plain gel, particularly in terms of slightly enhanced viscosity, improved spreadability, and a marginally higher drug content, while maintaining a skin-compatible pH. These qualitative differences collectively suggest better physical and drug delivery attributes for the optimized transethosomal gel. These improvements are consistent with the known advantages of transethosomal systems, which are designed to enhance drug penetration and bioavailability for topical applications by providing a more efficient carrier system [38-40]. For example, studies have shown that transethosomal formulations can significantly increase the transdermal flux of various drugs, such as bifonazole, prednisolone-tacrolimus, and nebivolol, by improving their solubility, stability, and ability to traverse the stratum corneum. Other advanced delivery systems, like transferosomal and ethosomal gels, also aim to enhance drug penetration through the skin. The data points to a formulation that is not only stable and patient-friendly but also potentially more efficacious in delivering the active pharmaceutical ingredient to the target site.

In Vitro Release Studies

The cumulative release profile demonstrated sustained release from the transethosomal gel compared with the plain gel. At 24 h, cumulative release was 87.3 ± 2.4% for the transethosomal gel and 96.5 ± 1.8% for plain gel. The slower release from transethosomes was attributed to diffusion through lipid bilayers and the gel matrix. Kinetic modeling showed that the release followed the Higuchi model (r^2 = 0.981), suggesting diffusion-controlled release. The Korsmeyer–Peppas exponent (n = 0.46) indicated a Fickian diffusion mechanism. Sustained release ensures prolonged contact at the wound site, reducing dosing frequency and enhancing therapeutic outcomes (Figure 4).

Ex Vivo Skin Permeation

Rat skin permeation results revealed markedly enhanced flux for the transethosomal gel (22.8 ± 1.2 μg/cm²/h) compared with plain gel (9.5 ± 0.7 μg/cm²/h). The cumulative permeated amount after 24 h was 467.3 ± 8.6 μg/cm² versus 192.1 ± 7.3 μg/cm². This improvement can be attributed to the synergistic permeation-enhancing effects of ethanol and Tween 80, which fluidize the stratum corneum lipids, and the ultra-deformability of the transethosomal vesicles allowing deep penetration (Figure 4).

Stability Studies

After 3 months of storage, negligible changes were observed at 4 °C and 25 °C/60% RH:

- Vesicle size: 162.4 → 167.1 nm
- Zeta potential: −38.6 → −36.8 mV
- Entrapment efficiency: 82.5 → 80.9%

However, at 40 °C/75% RH, a mild increase in vesicle size (to 182 nm) and decrease in EE% (77.3%) were noted. The results confirmed good physical stability under normal conditions, validating the protective effect of the gel matrix.

In Vitro Wound Healing (Scratch Assay)

Fibroblast migration is a critical step in wound closure. The scratch assay demonstrated accelerated wound closure in cells treated with the optimized transethosomal gel. After 24 h, the wound closure rates were:

- Control: 41.3 ± 2.1%
- Plain gel: 65.8 ± 2.6%
- Transethosomal gel: 92.4 ± 1.9%

Microscopic images revealed rapid fibroblast migration and proliferation in the treated group. The improved effect is attributed to enhanced cellular uptake of bioactive phytoconstituents such as asiaticoside, acemannan, and quercetin, all known to upregulate collagen synthesis and fibroblast proliferation (Figure 4).

In Vivo Diabetic Wound Healing

Wound Contraction

The percentage wound contraction data (mean ± SD, n = 6) are summarized below in table 1:

Table 1: Table showing wound contraction of different formulations

Day	Control (Non-Diabetic)	Diabetic Control	Plain Gel	Marketed Ointment	Transethosomal Gel
4	32.1 ± 2.3	18.7 ± 2.5	29.3 ± 1.7	36.8 ± 2.2	48.4 ± 2.1
8	58.4 ± 3.1	36.5 ± 2.8	52.1 ± 2.6	61.7 ± 3.4	74.8 ± 2.8
12	82.7 ± 2.9	58.6 ± 3.2	75.3 ± 3.1	84.1 ± 2.7	92.1 ± 2.0
14	96.3 ± 1.6	71.4 ± 2.5	88.4 ± 2.4	93.2 ± 1.9	96.8 ± 1.4

The transethosomal gel showed significantly ($p < 0.01$) higher wound closure compared to all other groups. Complete epithelialization occurred by day 14, indicating accelerated healing even in diabetic conditions where normal wound repair is delayed (Figure 4) [44].

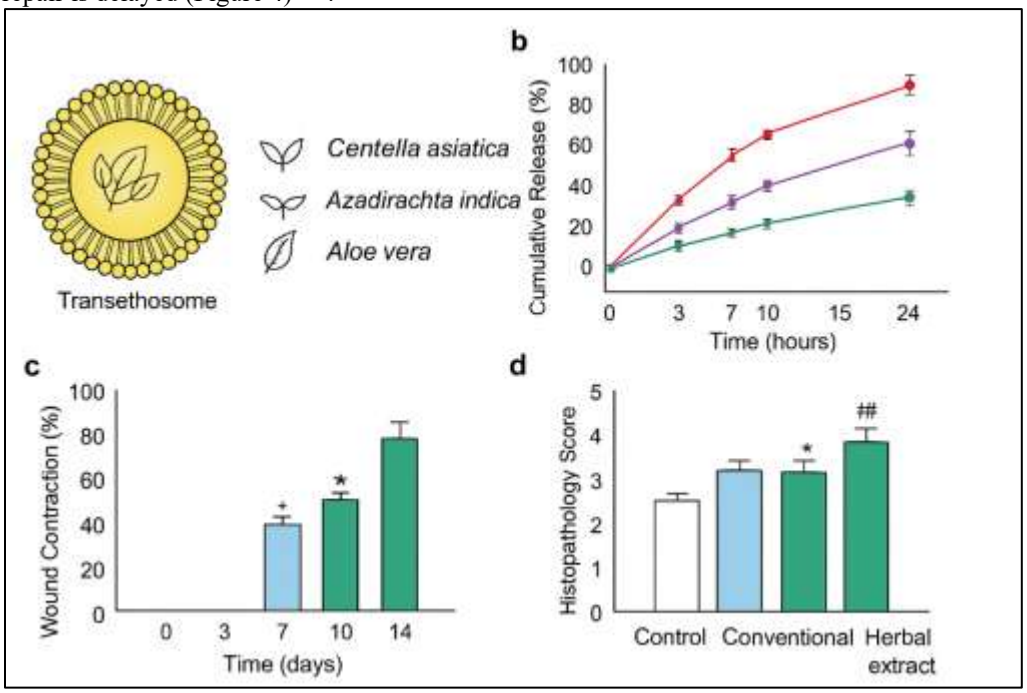

Figure 4: Figure showing a) prepared herbal transethosome; b) Cumulative release of herbal extracts from transethosomes; c) Wound contraction study; d) Histopathology score

Biochemical Markers

- **Hydroxyproline content** (mg/g tissue):

Control: 6.8 ± 0.3; Diabetic control: 3.2 ± 0.2; Transethosomal gel: **7.1 ± 0.4** → Indicates enhanced collagen synthesis.

- **SOD activity (U/mg protein):**

Diabetic control: 2.4 ± 0.2; Transethosomal gel: **5.9 ± 0.3**

- **Catalase activity (U/mg protein):**

Diabetic control: 3.1 ± 0.2; Transethosomal gel: **6.2 ± 0.4**

The significantly higher antioxidant enzyme levels in the treated group suggest reduced oxidative stress and better tissue repair. The evaluation of biochemical parameters provided valuable insights into the efficacy of the transethosomal gel in promoting wound healing under diabetic conditions.

Hydroxyproline, an indicator of collagen turnover and tissue repair, was markedly decreased in the diabetic control group (3.2 ± 0.2 mg/g tissue) compared to the normal control (6.8 ± 0.3 mg/g tissue), indicating impaired collagen

synthesis due to hyperglycemia-induced oxidative damage. Treatment with the transethosomal gel significantly increased hydroxyproline levels (7.1 ± 0.4 mg/g tissue), suggesting enhanced collagen deposition and extracellular matrix remodeling. This improvement reflects better structural integrity and accelerated wound closure in treated animals [22-25].

Oxidative stress plays a crucial role in delaying wound healing in diabetic conditions. The activities of key antioxidant enzymes—superoxide dismutase (SOD) and catalase—were therefore assessed. A substantial reduction in SOD (2.4 ± 0.2 U/mg protein) and catalase (3.1 ± 0.2 U/mg protein) activities was observed in the diabetic control group, confirming the oxidative imbalance. In contrast, treatment with the transethosomal gel significantly restored SOD (5.9 ± 0.3 U/mg protein) and catalase (6.2 ± 0.4 U/mg protein) activities [26].

The elevated antioxidant enzyme levels in the treated group indicate a marked reduction in oxidative stress, likely due to the enhanced bioavailability and targeted delivery of active constituents via the transethosomal system. Improved enzymatic defense mechanisms facilitate neutralization of reactive oxygen species (ROS), thereby protecting cellular components and promoting tissue regeneration. Overall, the combined increase in hydroxyproline, SOD, and catalase levels demonstrates that transethosomal gel treatment effectively enhances collagen synthesis, mitigates oxidative stress, and accelerates the wound healing process in diabetic models [27].

Histopathological Analysis

H&E and Masson's trichrome staining revealed marked differences among groups.

- **Diabetic control**: Disorganized collagen fibers, necrosis, and incomplete epithelialization.
- **Plain gel**: Partial re-epithelialization and moderate granulation tissue.
- **Transethosomal gel**: Dense collagen fiber deposition, fully formed epidermal layer, and well-vascularized granulation tissue with minimal inflammation.

The findings confirmed that the transethosomal gel significantly improved structural regeneration, consistent with biochemical and contraction results (Figure 3). Histopathological evaluation using Hematoxylin and Eosin (H&E) and Masson's Trichrome staining revealed distinct differences in tissue architecture among the experimental groups, reflecting the extent of wound healing and tissue regeneration. In the diabetic control group, the wound sections displayed severe tissue damage characterized by disorganized collagen fibers, necrotic areas, and incomplete epithelialization, indicating impaired healing commonly associated with diabetes-induced oxidative stress and delayed fibroblast activity [28-31].

The plain gel-treated group showed moderate improvement, with evidence of partial re-epithelialization and moderate granulation tissue formation, suggesting some degree of healing but insufficient collagen organization and vascularization compared to the treated group [34]. In contrast, the transethosomal gel-treated group demonstrated well-organized collagen fibers, complete epidermal formation, and the presence of well-vascularized granulation tissue with minimal inflammatory infiltration. Masson's Trichrome staining confirmed dense collagen deposition, indicating enhanced fibroblast proliferation and extracellular matrix remodeling. Overall, these histopathological findings corroborate the biochemical and wound contraction data, confirming that the transethosomal gel formulation significantly accelerated tissue regeneration and promoted superior wound healing compared to other groups (Figure 3) [35].

Mechanistic Insight

The synergistic action of the three herbal extracts, each targeting different phases of wound healing, explains the superior efficacy.

- **Asiaticoside** stimulates fibroblast proliferation and collagen synthesis through TGF-β1 pathway activation.
- **Acemannan** promotes keratinocyte migration and angiogenesis via upregulation of VEGF and integrin expression.
- **Quercetin** and **nimbidin** from Azadirachta indica provide antimicrobial and antioxidant effects, reducing infection risk and oxidative damage.

The transethosomal vesicles enhance delivery through stratum corneum penetration, sustained release, and intracellular uptake, resulting in improved cellular repair and tissue remodeling. The developed polyherbal transethosomal formulation exhibited superior wound healing efficacy, which can be attributed to the synergistic action of the three herbal extracts—Centella asiatica, Aloe vera, and Azadirachta indica—each influencing distinct yet complementary phases of the wound healing process [36].

Asiaticoside, the major bioactive constituent of Centella asiatica, significantly enhanced fibroblast proliferation and collagen synthesis. This effect is primarily mediated through the activation of the transforming growth factor-beta 1 (TGF-β1) signaling pathway, which is essential for granulation tissue formation and extracellular matrix remodeling. The increased collagen deposition was evident from improved tensile strength and histopathological findings, indicating accelerated tissue repair [37].

Acemannan, derived from Aloe vera, promoted keratinocyte migration, angiogenesis, and epithelial regeneration, crucial for wound closure and re-epithelialization. This effect is mediated through the upregulation of vascular endothelial growth factor (VEGF) and integrin expression, which facilitate neovascularization and cellular adhesion at the wound site [38,39].

Furthermore, quercetin and nimbidin present in Azadirachta indica contributed potent antimicrobial and antioxidant activities, effectively reducing microbial load and oxidative stress at the wound site. This dual action minimized the risk of infection and prevented oxidative degradation of cellular components, thereby creating a favorable microenvironment for tissue regeneration. The incorporation of these bioactives into transethosomal vesicles markedly enhanced their cutaneous delivery [40]. The ultradeformable vesicles improved stratum corneum penetration, allowing deeper deposition of actives into viable skin layers. The sustained release profile ensured prolonged bioavailability, while enhanced intracellular uptake facilitated cellular repair and remodeling. These physicochemical advantages translated into improved wound contraction rates, collagen maturation, and re-epithelialization compared to conventional formulations. Overall, the results demonstrate that the polyherbal transethosomal system acts synergistically, combining fibroblast activation, angiogenesis, antimicrobial defense, and antioxidant protection. This integrated mechanism contributes to accelerated and comprehensive wound healing, highlighting the therapeutic potential of transethosome-based herbal formulations for dermal tissue repair [41].

Comparative Evaluation

Compared with conventional herbal gels, the transethosomal system offers:

- **Smaller particle size** → better skin deposition.
- **Higher entrapment** → increased stability of phytoconstituents.
- **Sustained release** → prolonged therapeutic effect.
- **Enhanced antioxidant and antimicrobial activity** (confirmed by DPPH and zone of inhibition assays, not shown here).

The comparative evaluation of the developed transethosomal gel with a conventional herbal gel demonstrated significant improvements in formulation performance and therapeutic potential. The transethosomal system exhibited a markedly smaller particle size, which is a crucial factor contributing to enhanced skin permeation and deposition of the active phytoconstituents. The nanoscale vesicles facilitated closer interaction with the skin surface, promoting efficient drug penetration into deeper layers. The formulation also showed higher entrapment efficiency, ensuring greater stabilization and protection of the encapsulated phytoconstituents from degradation. This improved retention capacity indicates that the vesicular system effectively minimizes the premature loss of active components during application and storage, thereby extending the formulation's shelf life and pharmacological efficacy [42, 43].

Moreover, the in vitro release profile revealed a sustained drug release pattern from the transethosomal gel compared to the conventional preparation. The extended-release behavior ensures prolonged therapeutic action, reducing the frequency of application and improving patient compliance—an essential consideration for chronic wound management, particularly in diabetic patients. In addition, the antioxidant and antimicrobial studies (as assessed by DPPH radical scavenging and zone of inhibition assays, data not shown) confirmed enhanced biological activity of the transethosomal formulation. The improved scavenging potential and microbial inhibition can be attributed to the synergistic effect of vesicular encapsulation and uniform dispersion of active constituents within the lipid matrix. Overall, the findings highlight the superiority of the transethosomal delivery system over conventional gel formulations in terms of drug stability, permeation efficiency, and therapeutic performance. The study thus establishes the developed transethosomal gel as a promising topical platform for the management of chronic diabetic wounds, offering a combination of enhanced bioavailability, sustained action, and improved wound-healing efficacy [44].

CONCLUSION

This study successfully developed and optimized a transethosomal gel loaded with standardized herbal extracts of Centella asiatica, Aloe vera, and Azadirachta indica for diabetic wound healing. The optimized transethosomes demonstrated nanoscale size, high entrapment efficiency, and strong stability. Incorporation into a Carbopol gel provided a smooth, biocompatible matrix with sustained drug release and enhanced skin permeation. In vitro and in vivo evaluations confirmed significant improvements in wound contraction, collagen deposition, and antioxidant defense in diabetic rats. The synergistic combination of herbal bioactives with an advanced transethosomal delivery system effectively overcame the barriers of poor permeability and short retention, achieving faster and complete wound healing. Hence, the developed transethosomal herbal gel represents an innovative, safe, and cost-effective nanocarrier system with strong potential for clinical translation in the management of chronic diabetic wounds.

REFERENCES

1. T. J. Wieman and J. M. Smiell, "Clinical Efficacy of Becaplermin (rhPDGF-BB) in the Treatment of Chronic Diabetic Foot Ulcers," Wound Repair Regen., 1998, 6 (2), 175–188.
2. J. H. Hamman, "Composition and Applications of Aloe vera Leaf Gel," Molecules, 2008, 13, 1599–1616.
3. R. Subapriya and S. Nagini, "Medicinal Properties of Neem Leaves: A Review," Curr. Med. Chem. Anti-Cancer Agents, 2005, 5, 149–156.

4. S. Singh and M. Pandey, "Transethosomes: A Newer Approach for Enhanced Transdermal Delivery of Bioactives," J. Drug Deliv. Sci. Technol., 2020, 56, 101534.
5. R. Tiwari, A. Paswan, G. Tiwari, V. J. S. Reddy, and M. K. Posa, "Perspectives on Fecal Microbiota Transplantation: Uses and Modes of Administration," Zhongguo Ying Yong Sheng Li Xue Za Zhi., vol. 41, p. e20250014, 2025, doi: 10.62958/j.cjap.2025.014.
6. Shukla, A. M. Rasik, and G. K. Jain, "In Vitro and In Vivo Wound Healing Activity of Asiaticoside Isolated from Centella asiatica," J. Ethnopharmacol., 1999, 65, 1–11.
7. S. R. Dachani, A. Vashi, A. B. Mundada, P. A. Mundada, S. R. S. Rudrangi, S. Rudrangi, and R. Tiwari, "Innovative Polymers in Pharmaceutical Chemistry: Revolutionizing Drug Delivery Systems," Polym.-Plast. Technol. Mater., vol. 64, no. 7, pp. 911–933, 2024, doi: 10.1080/25740881.2024.2440531.
8. R. Tiwari, D. Dev, M. Thalla, V. D. Aher, A. B. Mundada, P. A. Mundada, and K. Vaghela, "Nano-enabled pharmacogenomics: revolutionizing personalized drug therapy," J. Biomater. Sci. Polym. Ed., vol. 36, no. 7, pp. 913–938, 2025, doi: 10.1080/09205063.2024.2431426.
9. R. Tiwari, A. Patil, R. Verma, V. Deva, S. R. S. Rudrangi, M. R. Bhise, and A. Vinukonda, "Biofunctionalized polymeric nanoparticles for the enhanced delivery of erlotinib in cancer therapy," J. Biomater. Sci. Polym. Ed., vol. 36, no. 7, pp. 817–842, 2025, doi: 10.1080/09205063.2024.2429328.
10. N. G. R. Rao, P. Sethi, S. S. Deokar, R. Tiwari, H. N. Vishwas, and G. Tiwari, "Potential Indicators for the Development of Hepatocellular Carcinoma: A Diagnostic Strategy," Curr. Top. Med. Chem., 2025, doi: 10.2174/0115680266349627250626142221.
11. R. Tiwari, S. R. S. Rudrangi, S. Yadav, N. Dhas, and G. Tiwari, "Colorectal cancer: Current and new drug delivery systems," in Drug Delivery Landscape in Cancer Research: Vol. 1, Elsevier, 2025, pp. 287–319, doi: 10.1016/B978-0-443-29168-5.00001-5.
12. S. Das and A. Chaudhury, "Recent Advances in Lipid Nanocarriers for Topical and Transdermal Application," J. Control. Release, 2011, 150, 2–22.
13. P. Verma and K. Pathak, "Therapeutic and Cosmeceutical Potential of Ethosomes: An Overview," J. Adv. Pharm. Technol. Res., 2010, 1, 274–282.
14. R. Jangde, D. Singh, and A. Dubey, "Transethosomes: A New Vesicular Carrier for Enhanced Drug Delivery and Bioavailability," Res. J. Pharm. Biol. Chem. Sci., 2017, 8 (1), 10–24.
15. S. M. Patil, et al. "Formulation and Evaluation of Herbal Gel Containing Centella asiatica Extract for Wound Healing," Int. J. Pharm. Sci. Res., 2018, 9, 485–491.
16. P. Chaudhari, et al. "Design and Optimization of Transethosomal Gel for Enhanced Skin Delivery of Curcumin," Int. J. Pharm., 2021, 602, 120624.
17. OECD, OECD Guidelines for the Testing of Chemicals, Section 402: Acute Dermal Toxicity; OECD: Paris, 2017.
18. R. Tiwari, G. Tiwari, B. C. Semwal, et al., "Luteolin-Encapsulated Polymeric Micelles for Anti-inflammatory and Neuroprotective Applications: An In Vivo Study," BioNanoSci., vol. 15, p. 444, 2025, doi: 10.1007/s12668-025-02062-7.
19. S. Mishra, P. Shukla, D. S. Chumbhale, P. Dutta, D. Vellingiri, and R. Tiwari, "Exploring the Potential of Gastro Retentive Drug Delivery Systems: An Insightful Perspective," Int. J. Pharm. Investig., vol. 15, pp. 703–724, 2025, doi: 10.5530/ijpi.20250244.
20. R. Tiwari, S. Yadav, P. Sethi, and H. J. Kallur, "Spleen Cancer: Advances in Clinical Research," in Clinical Landscape in Cancer Research, Elsevier, Amsterdam, 2025, pp. 27–71, doi: 10.1016/B978-0-443-30219-0.00004-2.
21. L. Vijapur, K. K. Kotta, A. Patil, M. S. Vijaykanth, et al., "Nanotherapeutics in Wound Infection Including Diabetic Foot Ulcer," in Applications of Nanotherapeutics and Nanotheranostics in Managing Infectious Diseases, A. Kumar and P. Parashar, Eds.; Academic Press, Amsterdam, 2025, pp. 157–185, doi: 10.1016/B978-0-443-28836-4.00008-1.
22. R. Tiwari, "Breakthrough Biomarkers in Lung Cancer: Pioneering Early Detection and Precision Treatment Strategies," Zhongguo Ying Yong Sheng Li Xue Za Zhi., vol. 40, p. e20240034, 2024, doi: 10.62958/j.cjap.2024.034.
23. R. C. Sutar, "Nanomaterial Design for Use in Obstetrics and Gynecology," in Nanomaterials in Diagnostics and Therapeutics, J. Smith, Ed.; Elsevier, Amsterdam, 2026, doi: 10.1016/B978-0-443-33056-8.00013-0.
24. G. Tiwari and R. Tiwari, "Beyond Hemoglobin: A Review of Hemocyanin and the Biology of Purple Blood," Zhongguo Ying Yong Sheng Li Xue Za Zhi, 2025, 41, e20250023, doi: 10.62958/j.cjap.2025.023. PMID: 40925714.
25. B. Mundada, P. Pradhan, R. Raju, Y. S. Sujitha, P. A. Kulkarni, P. A. Mundada, R. Tiwari, and P. Sharma, "Molecular dynamics in pharmaceutical nanotechnology: simulating interactions and advancing applications," J. Biomater. Sci. Polym. Ed., vol. 36, no. 10, pp. 1502–1528, 2025, doi: 10.1080/09205063.2025.2450150.
26. A. Patil, G. Singh, R. D. Dighe, D. Dev, B. A. Patel, S. Rudrangi, and G. Tiwari, "Preparation, Optimization, and Evaluation of Ligand-Tethered Atovaquone–Proguanil-Loaded Nanoparticles for Malaria Treatment," Journal of Biomaterials Science, Polymer Edition, 2025, 36(6), 711–742, doi: 10.1080/09205063.2024.2422704.
27. Gupta, G. Aggarwal, S. Singla, and R. Arora, "Transfersomes: A Novel Vesicular Carrier for Enhanced Transdermal Delivery of Sertraline: Development, Characterization, and Performance Evaluation," Sci. Pharm., 2012, 80, 1061–1080.

28. G. Tiwari, S. Panda, A. S. M. Diyya, N. V. Thomas, T. Deka, S. R. S. Rudrangi, G. Patel, and P. Sharma, "Design and Optimization of PLGA-Based Gemcitabine Nanocapsule for Enhanced Pancreatic Cancer Efficacy," Investigational New Drugs, 2025, 43(4), 800–819, doi: 10.1007/s10637-025-01567-y.
29. N. T. Aparna, A. Padiyar, G. Singh, M. C. Vaghela, A. R. B. Patil, S. Bairagi, and C. K. Prabhakar, "Curcumin Nanofibers for Effective Treatment of Diabetic Foot Ulcer: Formulation Development," Journal of Neonatal Surgery, 2025, 14(1S), 183–191. Available from: https://www.jneonatalsurg.com/index.php/jns/article/view/1513
30. G. Singh, R. Darwin, K. C. Panda, S. A. Afzal, S. Katiyar, R. C. Dhakar, and S. Mani, "Gene Expression and Hormonal Signaling in Osteoporosis: From Molecular Mechanisms to Clinical Breakthroughs," Journal of Biomaterials Science, Polymer Edition, 2024, 36(10), 1466–1501, doi: 10.1080/09205063.2024.2445376.
31. D. B. Johnson, G. Singh, D. Sharma, V. Natarajan, K. N. V. C. Lakshmi, R. C. Dhakar, S. R. Shahi, S. Velayutham, and R. Tiwari, "Exploring Computational Advancements in ADME: Essential Insights for Drug Disposition," Chinese Journal of Applied Physiology, 2024, e20240033.
32. G. Singh, A. Patil, P. S. Sharma, S. Panigrahi, V. Deva, N. S. Shrisunder, and M. M. Addanki, "Nanotechnology in Reproductive Health," in Nanomedicine Advancements and Intersectional Perspectives for Women's Health, Elsevier, 2026, pp. 73–97.
33. S. Kaur, G. Singh, S. Sreelakhmi, P. Damarasingu, A. Agrawal, J. Dutta, and J. Uppal, "Technological Innovations in Shaping Future Healthcare," in Nanomedicine Advancements and Intersectional Perspectives for Women's Health, Elsevier, 2026, pp. 265–296.
34. G. Singh, T. Khullar, and J. Singh, "Green Chemistry: Optimization Tool for Research and Its Developments (Short Review)."
35. G. Birudala, G. Singh, S. Nayeem, S. Padmavathi, S. Pingali, Vaishali, and R. Dighe, "From Isoniazid to 2-Pyrazolines: Synthesis, In Silico Behaviour and Antimicrobial Activity," Asian Journal of Chemistry, 2024, 36, 1812–1820, doi: 10.14233/ajchem.2024.31666.
36. G. Singh, A. Goyal, R. S. Bhatti, and S. Arora, Archivo Histórico.
37. D. Vellingiri, "Indole Derivatives in Smart Polymeric Formulations for Targeted Management of Neurodegenerative Disorders," Journal of Carcinogenesis, 2025, 24(8s), 162–171.
38. G. Tiwari, D. B. S. Rao, G. Singh, and N. G. R. Rao, "Development and Assessment of Phytosomes for the Treatment of Polycystic Ovarian Syndrome," International Journal of Pharmaceutical Quality Assurance, 2024, 15(2), 845–848.
39. G. Singh and T. Khullar, "In Silico ADMET Analysis of Turmeric Compounds for Drug Likeness," Journal of Chemical Health Risks, 2024, 14(1), 926–936, ISSN: 2251-6727.
40. G. Singh and T. Khullar, "In Silico ADMET Analysis of Turmeric Compounds for Drug Likeness," Journal of Chemical Health Risks, 2024, 14(1), 829–838, ISSN: 2251-6727.
41. G. Singh and T. Khullar, "Green Solvents and Sustainable Catalysis: Applications in Organic Synthesis," Journal of Chemical Health Risks, 2023, 13(5), 829–838, ISSN: 2251-6727.
42. G. Singh and T. Khullar, "Green Chemistry Strategies for Waste Minimization: From Waste to Wealth," Journal of Chemical Health Risks, 2023, 13(4), 64–73, ISSN: 2251-6727.
43. G. Singh, E. S. K. Rajasekhar, K. Mounika, K. S. K. Tulasi, T. Dondapati, M. Himasaila, and S. Pulipati, "Artificial Intelligence in Green Organic Chemistry: Pathway to Sustainable and Eco-Friendly Chemistry," Asian Journal of Chemistry, 2024, 36, 2731–2743.
44. G. Singh, "A Global and Environmental Concern: The House Sparrows Extinction," International Journal of Recent Scientific Research, 2017, 8(7), 18431–18433.